DOI: 10.1002/chem.201100515

Clustering of *Escherichia coli* Type-1 Fimbrial Adhesins by Using Multimeric Heptyl α-D-Mannoside Probes with a Carbohydrate Core

Mehdi Almant,[a] Vincent Moreau,[a] José Kovensky,[a] Julie Bouckaert,*[b, c] and Sébastien G. Gouin*[a, d]

Abstract: Heptyl α-D-mannoside (HM) is a strong inhibitor of the FimH lectin that mediates the initial adhesion of the uropathogenic *Escherichia coli* (*E. coli*) to the bladder cells. We designed a set of multivalent HM ligands based on carbohydrate cores with structural valencies that range from 1 to 7. The chemical strategy used to construct the regular hydrophilic structures consisted of the repetition of a critical glucoside fragment. A primary amino group was grafted at the sugar reducing end to couple the multimers to a fluorescent label. A one-pot synthetic approach was developed to tether the ligands and the fluorescein isothiocyanate (FITC) probe to the scaffold simultaneously. Isothermal calorimetry with the monomeric FimH lectin revealed nanomolar affinities and saturation of all structurally available binding sites on the multivalent HM ligands. Direct titrations domain showed almost strict correlation of enthalpy–entropy compensation with increasing valency of the ligand, whereas reverse titration calorimetry demonstrated negative cooperativity between the first and the second binding site of the divalent heptyl mannoside. A multivalency effect was nevertheless observed by inhibiting the haemagglutination of type-1 piliated UTI89 *E. coli*, with a titer as low as 60 nM for the heptavalent HM ligand. An FITC-labeled HM trimer showed capture and cross-linking of living bacteria in solution, a phenomenon not previously described with low-valency ligands.

Keywords: calorimetry · carbohydrates · click chemistry · clusters · multivalency

Introduction

The development of bacterial strains that are multiresistant to antibiotic treatments is a serious health problem that is getting worse. This is partially due to the widespread prescriptions of antibiotics and their use in animals and agriculture.[1] In parallel, the antimicrobial developments continue to stagnate and the actual research programs may be unable to provide an efficient solution in the next decade.[2] Nowadays, at least one mechanism of resistance has been identified for each class of antibiotics, and we are currently witnessing highly resistant strains emerging around the world.[3] There is an urgent need for the development of antibiotics with new mechanisms of action and of alternative therapeutics that are less prone to give rise to antibiotic resistance. An appealing strategy envisioned by a part of the scientific community is the development of anti-adhesive drugs that are able to prevent bacterial attachment to the host cells. Bacterial adhesion is generally promoted by proteins named adhesins that bind to the carbohydrates displayed on the surface of the host cells. Interfering with pathogen adhesion is an attractive alternative, because the bacteria are not killed and thus are less prone to develop resistance. A large set of glycomimetics with different structures have been designed by chemists to interfere with early stages of bacterial infection.[4] Glycomimetics generally display several copies of the ligands for the lectin on a common scaffold. The affinity enhancement observed for such systems can be much higher than expected from the sum of the constitutive interactions, a phenomenon referred to as the "multivalent or glycoside cluster effect."[5]

We recently focused our efforts on the development of inhibitors of virulent strains of the Gram-negative bacterium *Escherichia coli*, associated with urinary tract infections

[a] Dr. M. Almant, Dr. V. Moreau, Prof. J. Kovensky, Dr. S. G. Gouin
Laboratoire des Glucides UMR CNRS 6219
Institut de Chimie de Picardie, UFR des Sciences
Université de Picardie Jules Verne
33 rue Saint-Leu, 80039 Amiens Cedex 1 (France)

[b] Dr. J. Bouckaert
Unité de Glycobiologie Structurale et Fonctionnelle
UMR CNRS 8576
Université des Sciences et Technologies de Lille 1
59, 655 Villeneuve d'Ascq (France)
Fax: (+33) 320436555
E-mail: Julie.Bouckaert@univ-lille1.fr

[c] Dr. J. Bouckaert
Molecular recognition, Vrije Universiteit Brussel
Pleinlaan 2, 1050 Brussels (Belgium)

[d] Dr. S. G. Gouin
Present address: Université de Nantes
Chimie et Interdisciplinarité, Synthèse, Analyse,
Modélisation (CEISAM), UMR CNRS 6230
UFR des Sciences et des Techniques
2, rue de la Houssinière, BP 92208
44322 Nantes Cedex 3 (France)
Fax: (+33) 251125712
E-mail: sebastien.gouin@univ-nantes.fr

Supporting information for this article is available on the WWW under http://dx.doi.org/10.1002/chem.201100515.

(UTIs). Initial attachment of the pathogens to the bladder cells is mediated by a mannose-specific adhesin named FimH, situated at the edge of the tip fibrillum of type-1 fimbriae. Simultaneous binding of several fimbriae to mannosides displayed by the glycoprotein uroplakin Ia allows for a tight binding of the bacteria to the uroepithelial cells. Previous results have also shown that inhibition of type-1 fimbriated *E. coli* can be efficiently achieved with synthetic monovalent mannosides that bear hydrophobic aglycons in the anomeric position such as aryl groups.[6–8] Hultgren and coworkers have recently identified a biaryl mannoside that displays low nanomolar binding affinity and submicromolar cellular activity in a fluorescence polarization and haemagglutination assay, respectively.[9] Interestingly, simpler alkyl mannosides were also shown to be strong binders of the FimH protein.[10] With a binding affinity of 5 nM recorded by surface plasmon resonance (SPR), and the ability to reduce the bacterial level in vivo, heptyl α-D-mannoside (HM) was identified as a promising potential anti-adhesive drug.[11]

Synthetic multimeric mannosides were also designed to generate more potent anti-adhesive drugs through the glycoside cluster effect. The chemical strategies reported generally consist of tethering simple mannoside ligands to functionalized cores such as dendrimers,[12] nanoparticles[13,14] and polymeric materials,[15,16] thereby leading to glycoclusters with specific valencies, architectures, and epitopes densities. The observed multivalent effects and enhanced affinities with type-1 fimbriated *E. coli* are generally limited compared to the gain reported when grafting anomeric lipophilic aglycons.[17] Such a trend was observed by Roy and colleagues with mannosylated neoglycoproteins and dendrimers.[12]

We also explored in our group the possibility of making potent anti-adhesive drugs by applying the concept of multivalency to strong monovalent FimH inhibitors. We designed multimeric HM with structural valencies that ranged from 1 to 4 on a carbohydrate scaffold and identified a tetramer that inhibited the bacterial bladder cell binding at a 64-fold lower concentration than HM.[18] The derivative was the most potent anti-adhesive compound evaluated by this assay toward uropathogenic *E. coli*. Although the synthetic strategy was straightforward, it was not applicable to the design of higher-valency compounds. Binding assays were also limited, as the set of multimers lacked an additional functional group for grafting onto a surface or chemical coupling to a fluorescent probe.

Carbohydrates are particularly appealing scaffolds for the design of glycoclusters. The hydroxyl groups can be selectively functionalized, and we and others have used this feature to modulate the topology of the ligands of carbohydrate-centered glycosides.[19–22] The highly hydrophilic core also prevents potential solubility problems due to the presence of hydrophobic substituents. We present here a protocol for the synthesis of mono, di-, tri-, and heptavalent HM based on a carbohydrate scaffold (Scheme 1). Differences in affinity will be reported relative to the monovalent derivative that bears the glucoside fragment and the triazole ring.

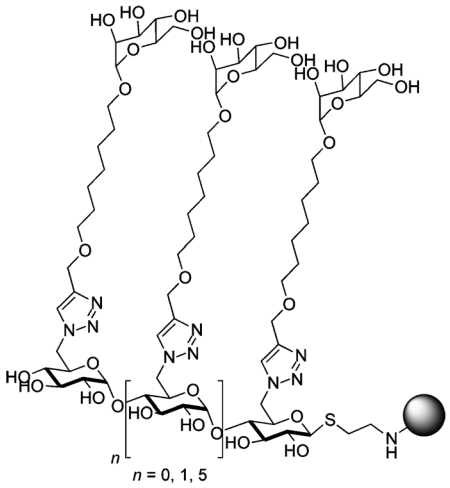

Scheme 1. Chemical structure of the HM glycoconjugates.

This reference is more appropriate than generally used methyl mannoside to take into account direct interactions of the aglycon groups with FimH. In such a regular system, the modulation of valency does not introduce new functional groups or affect the hydrophilicity or the spatial presentation of HM epitopes, because a critical fragment is repeated *n* times. This is of importance to strictly assess how the valency of the ligand influences lectin and bacterial binding. The binding mode of the multimers with FimH was measured by isothermal titration calorimetry (ITC). Binding affinities of synthetic glycoclusters toward type-1 piliated *E. coli* were evaluated by inhibition of haemagglutination (HAI). Fluoresceine isothiocyanate (FITC) was grafted onto a trimer to assess whether a low-valency ligand can aggregate bacteria in solution.

Results and Discussion

Glucose **1**, maltose **3**, and maltotriose **4** were used as scaffolds to generate the mono-, di-, and trivalent HM ligands. The copper-catalyzed azide–alkyne cyclization (CuAAC) was selected to graft alkynyl-armed HM epitopes onto azido-functionalized carbohydrate cores.[23] This reaction owes its usefulness due to its high efficiency and selectivity in different solvent systems including water.[24] Furthermore, numerous recent examples successfully report the use of CuAAC to design glycoclusters and other sugar mimetics.[25,26] Compound **2** was obtained in three synthetic steps as previously described in the literature (Scheme 2).[27] Tosylation of unprotected glucose in the C-6 position followed by acetylation of the hydroxyl groups and substitution by an azide efficiently provided gram-scale quantities of **2**. Maltose **3** and maltotriose **4** were functionalized with a procedure that we previously developed for the selective azidation of unprotected carbohydrates.[28] The protocol used a $PPh_3/CBr_4/NaN_3$[29] mixture in a 2:2:10 ratio relative to the sugar unit, followed by acetylation of the crude mixture. An alternative consists of a selective chloration of the C-6 car-

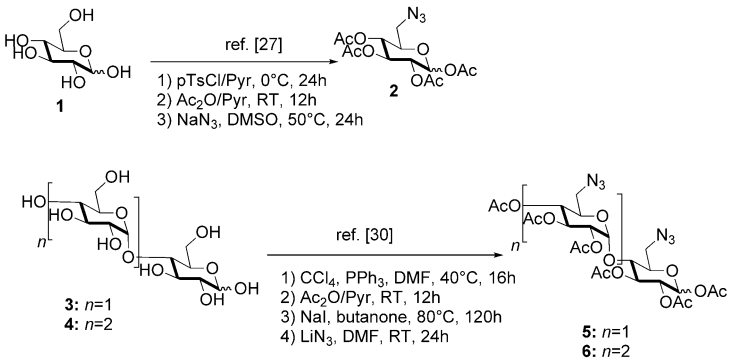

Scheme 2. Azidation of saccharides.

bons, acetylation of the hydroxyl groups, and two successive nucleophilic displacements by sodium iodide and azide.[30] Although this last procedure is much longer and requires additional purification steps, it allows the preparation of **5** and **6** in higher scales.

Carbohydrate cores with additional numbers of sugar units are particularly difficult to functionalize in a selective and quantitative way. Development of an efficient methodology is also hampered by the high cost of the corresponding commercial sugars. To our knowledge, there are no reports of the direct and selective halogenation or tosylation on the C-6 position of linear oligosaccharides.

On the contrary, the selective halogenation of the lower rim of cyclomaltooligosaccharides (α-, β-, and γ-cyclodextrins, CDs) is relatively straightforward and has been previously reported.[31–33] The per-6-bromo-β-CD **7** was first prepared in good yields with the Vilsmeier–Haack reagent $[(CH_3)_2NCHBr]^+Br^-$.[33] Subsequent per-acetylation with acetic anhydride and per-benzoylation with benzoyl bromide followed by nucleophilic substitution with sodium azide allowed isolation of the compounds **8** and **9**, respectively.[34]

Several methodologies are reported to form the linear malto-oligosaccharide from the corresponding CDs with Lewis or Brønsted acids such as H_2SO_4/Ac_2O,[35] $FeCl_3/Ac_2O$,[36] $ZnBr_2/PhSSiMe_3$,[37] $HClO_4/Ac_2O$,[38,39] $TiCl_4$, or $BF_3/MeOCH_2CO_2H$.[40] These different protocols were evaluated on the acetylated derivative **8** without any success. The expected linear heptasaccharide was only formed with H_2SO_4/Ac_2O[35] and in a low yield (less than 10%) due to the formation of shorter linear oligomers by a depolymerization process. Finally, the ring opening was performed with a good yield of 85% starting from the benzoylated derivative **9** (Scheme 3). The reaction was performed with the $HClO_4/Ac_2O$ mixture and at a low temperature of −20°C to avoid the formation of shorter oligosaccharides.

With the azido compounds **2**, **5**, **6**, and **10** in hand, we next focused on the introduction of the protected amino group in the anomeric position. A direct thioglycosylation with previously described 9-fluorenylmethoxycarbonyl (Fmoc)-protected cysteamine **15**[41] and **2**, **5**, **6**, and **10** was first considered. Unfortunately, no reaction occurred with the set of Lewis acids tested ($BF_3{\cdot}OEt_2$, trimethylsilyl trifluoromethanesulfonate (TMSOTf), $SnCl_4$, $[MoO_2Cl_2]$[42]) due to the oxidation of thiol **15** to the corresponding disulfide. Compounds **2**, **5**, **6**, and **10** were then converted in two steps to the corresponding trichloroacetamidates **11**, **12**, **13**, and **14** with an overall yield of 80, 73, 80, and 65%, respectively. Thioglycosylation occurred with the Schmidt procedure by using an excess amount of protected cysteamine and TMSOTf as catalyst. Expected compounds **16**, **17**, **18**, and **19** were obtained with fair yields of 75, 65, 55, and 35%, respectively. The reactions should be conducted at low temperature (−20°C) to avoid the partial formation of α anomers. The CuAAC reactions were performed under microwave irradiation with the

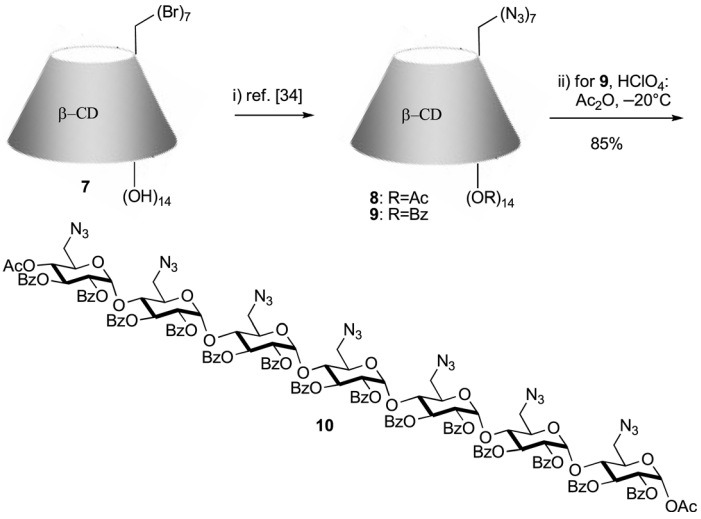

Scheme 3. Ring opening of cyclodextrin **9**.

previously described mannoside **20**.[18] The protocol allowed the fast formation of the expected cycloadducts **21**, **22**, and **23** with yields of 80, 73, and 76% respectively. The large $\Delta(\delta_{C-4}-\delta_{C-5})$ values ($\delta > 20$ ppm) observed by ^{13}C NMR spectroscopy for the different structures indicated the exclusive formation of the 1,4-cycloadducts, as smaller values are expected for 1,5-disubstitued regioisomers.[43]

Quantitative cleavage of the Fmoc, acetyl, or benzoyl groups were finally performed in a one-step procedure with a 7N solution of ammonia in methanol. Heptasaccharide **19** was subjected to the cyclization step and the crude product directly deprotected to **27**. The set of deprotected compounds **24**, **25**, **26**, and **27** (Scheme 4) were purified by HPLC on a C18 column.

We decided to graft a fluorescent dye onto **26** to assess its capacity to aggregate *E. coli* in solution. Commercially available fluorescein isothiocyanate was grafted on the trivalent ligand **26** in DMF, and subsequent purification by HPLC allowed isolation of the expected fluorescent ligand **30** (Scheme 5).

In parallel, we wanted to assess the possibility of performing an unprecedented one-pot coupling of the HM ligands and FITC probe to the carbohydrate scaffolds. Fmoc and acetyl groups of compound **18** were then deprotected at

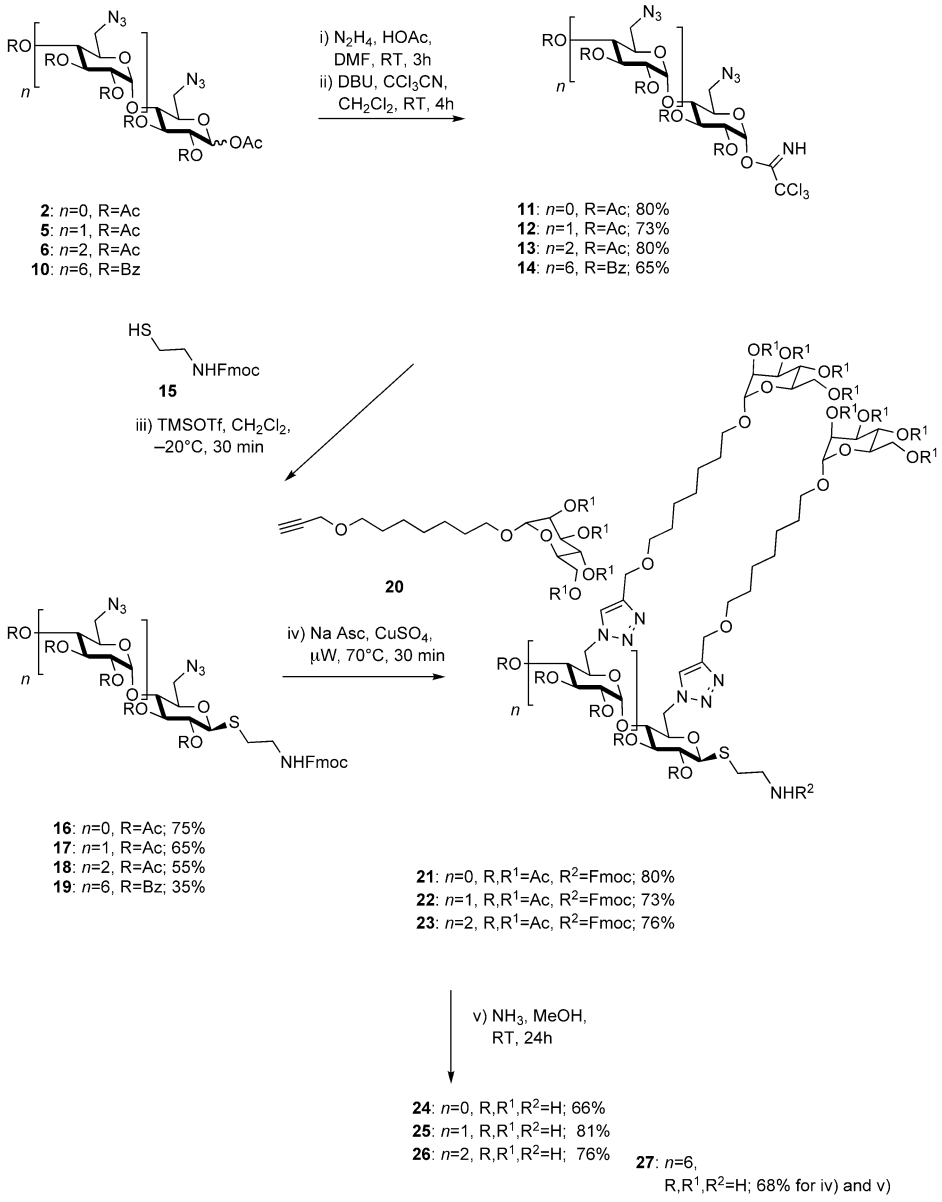

Scheme 4. Synthesis of cycloadducts **24**–**27**.

room temperature in methanolic ammonia to lead to crude compound **28**. Dissolution of the unprotected scaffold **28** in a DMF/water mixture with unprotected HM ligand **29**, FITC, and a catalytic quantity of copper sulfate and sodium ascorbate afforded the expected probe **30** within 35% yield after HPLC purification (Scheme 6).

Inhibition of haemagglutination (HAI): Binding affinities of the glycoconjugates **24**–**27** for type-1 piliated UTI89 clinical isolate *E. coli* were evaluated by HAI. Interaction of *E. coli* FimH adhesins with the glycocalyx of guinea pig erythrocytes formed a cross-linked network into the wells. Subsequent additions of HM or glycoconjugates **24**–**27** in a two-fold dilution series prevented the agglutination reaction. The inhibition titer is defined as the lowest concentration of the glycoconjugate at which haemagglutination is still inhibited (Table 1). Due to serial dilutions, the maximal error is ± 1 well, or a factor of two. HM, one of the most potent FimH inhibitors reported to date, was used as a reference compound. Monovalent derivate **24** was identified as a strong inhibitor within the same concentration range as HM (Table 2). More importantly, a significant enhancement was observed with the multimers **25**, **26**, and **27**. Potency increases with valency, and the heptavalent compound **27** is a 64-fold better inhibitor than HM, which means a ninefold improvement when reported on a mannose molar basis. Thus, there is a enhancement of the valency of the ligand on bacteria-mediated red blood agglutination. This can only be explained by the capacity of multivalent **25**, **26**, and **27** to cross-link different FimH molecules on pili of adjacent *E. coli*. Compared to our previously described multivalent HM derivatives based on oligoethylene glycol scaffolds, **25**, **26**, and **27** displayed higher affinity enhancements by HAI when reported on a mannose molar basis. This highlights the importance of a careful core selection for the design of FimH inhibitors. With the very low titer of 60 nM, **27** is to our knowledge the most potent FimH inhibitor identified by this assay.

Finally, the increasing titer potency and multivalent effect relative to mannosides epitopes from **24** to **27** also suggest that ligands with higher valencies based on a similar architecture would be even more potent inhibitors.

Table 1. HAI of HM and synthetic glycoconjugates **27**–**30**.

Compound	Valency	Titer [μM]	Ratio [L/HM]	Pot [M]
HM	1	4	1	1
24	1	4	1	1
25	2	0.5	8	4
26	3	0.25	16	5
27	7	0.06	64	9

Isothermal titration calorimetry: The affinities of the multivalent mannosides **24**, **25**, **26**, and **27** towards the FimH ad-

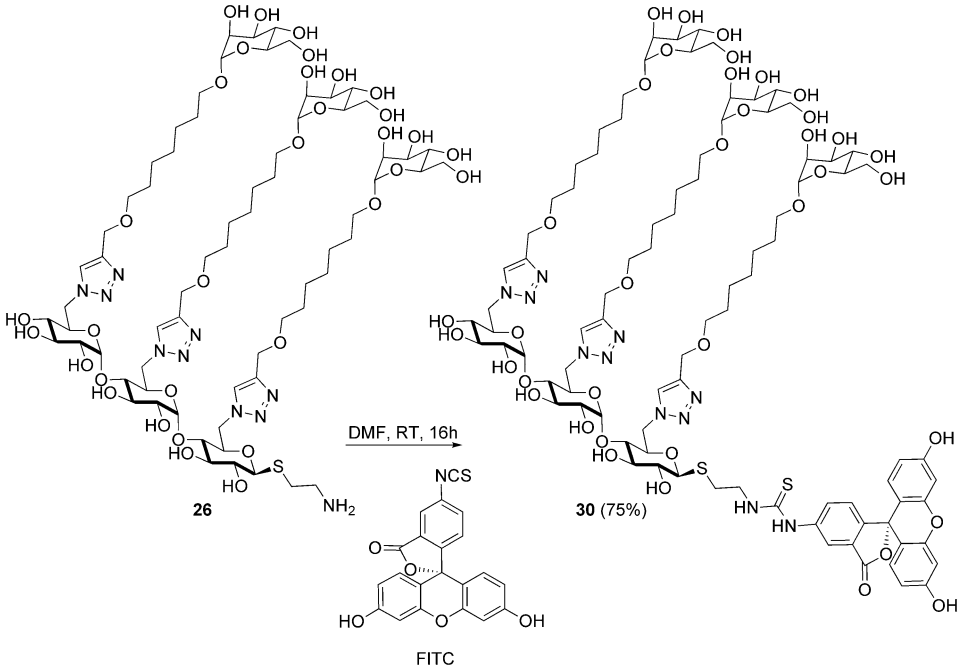

Scheme 5. Synthesis of probe **30**.

Table 2. ITC data for glycoconjugates **24**–**27** to the soluble, monomeric FimH lectin.

Cpd	n^{str}	K_d[a] [nM]	$\Delta G°$ [kcal mol^{-1}]	$\Delta H°$[a] [kcal mol^{-1}]	$\Delta S°$ [cal mol^{-1} K^{-1}]	$\chi^2/^{DOF}$[c]	n^{fun}
24	1	14.4 (±3.4)	−10.6	−10.1 (±0.1)	1.5	7.2×10^4	0.97
25	2	2.6 (±1.7)	−11.6	−16.6 (±0.2)	−16.9	1.5×10^5	0.46
25[d]	1/2	7.6 (±14.4)	−11.0	−14.3 (±0.7)	−11.1	3.5×10^6	1.00
25[d]	2/2	2128 (±7696)	−7.7	−3.3 (±5.9)	14.8	3.5×10^6	1.00
26	3	2.4 (±2.6)	−11.8	−43.6 (±1.3)	−108	7.2×10^6	0.31
27[b]	7	36.2 (±22.7)	−10.2	−68.3 (±4.2)	−197	1.3×10^8	0.15

[a] Standard deviations are in parentheses. [b] Average over two direct titration measurements. [c] Degree of fitting. [d] Divalent compound **25** was measured both using direct and reverse titration, the reverse tritration displaying the individual binding parameters for binding to the first (1/2) and the second (2/2) mannoside on **25**. The n^{str} value is the structural valency of the compound; n^{fun} is the molar ratio of monomeric FimH lectin domain over the compound, or the inverse of the functional valency of the glycoconjugates. The Gibbs free energy for the interaction is calculated as $\Delta G° = \Delta H° - T\Delta S°$, with T being the absolute temperature during the ITC measurement.

hesin have been assessed using isothermal titration calorimetry (VP-ITC instrument, Microcal). In a series of direct titrations, the FimH lectin domain was placed in the cell and the ligands were titrated into the cell through the needle (Figure 1).

As can be seen from Table 2, the number of FimH lectins bound per molecule, or the functional valency n^{fun}, increases congruently with the structural valency n^{str} of the glycoconjugates. Approximately two FimH lectin domains bind to the divalent ligand **25**, three FimH molecules per trivalent derivative **26** and seven FimHs were found to bind to the heptavalent **27**. It therefore seems that the close proximity of the clustered ligands does not prevent the simultaneous binding of FimH lectins and that ultimately all structural binding sites on the multivalent ligand can be saturated by FimH. These results are in accordance with ITC experiments recently reported with dodecamannosylated fullerenes that were shown to be able to accommodates up to seven FimH molecules relative to the twelve mannosides displayed on the scaffold.[44] Compared to the mannose-functionalized fullerenes, the topological distribution of the mannoside residues in **27** seems more favorable for cross-linking FimH molecules. We expect this distribution to follow a left-handed helix with regards to the nature of the carbohydrate core that consists of glucose residue with α(1→4) glycosidic bonds, similarly to amylose.[45]

The dissociation constants, K_d, in Table 2 indicated that the synthetic glycoconjugates are nanomolar inhibitors of FimH. There is an initial improvement in affinity for FimH going from the monomeric compound **24** to the dimeric ligand **25** and trimeric compound **26**. The trimeric ligand **26** displayed the steepest transition in the direct titration curve, which was related to a maximal affinity measureable by a normal direct titration. The affinity decreases again for the heptavalent **27**, in apparent contradiction with the potency of **27** in preventing the haemagglutination by the uropathogenic *E. coli* (Table 1). However, contrary to haemagglutination, strong affinity enhancements were not expected in the ITC measurements because of the monomeric nature of the FimH lectin. In bacterial cross-linking on the multivalent ligands, the FimH adhesin binds tightly to HM and aggregates closely together with the other FimH lectins onto the soluble carbohydrate scaffold. The larger the functional valency of the ligand, the larger these microclusters of FimH grow. Increasing noise levels were indeed observed in the ITC experiments from the monovalent compound **24**, over the bi- (**25**) and trivalent (**26**) ligands, to the heptavalent **27** (Figure 1 and Table 2 ($\chi^2/^{DOF}$)). Successive protein–protein attractions and repulsions within these microclusters could cause small heat releases and heat uptakes, respectively. The integration of the heat release upon each injection over the equilibration period may thus vary more considerably for compounds with higher ligand valencies. However, here these signals are not indicative of significant protein precipitation and the overall integrated enthalpy of the reaction is

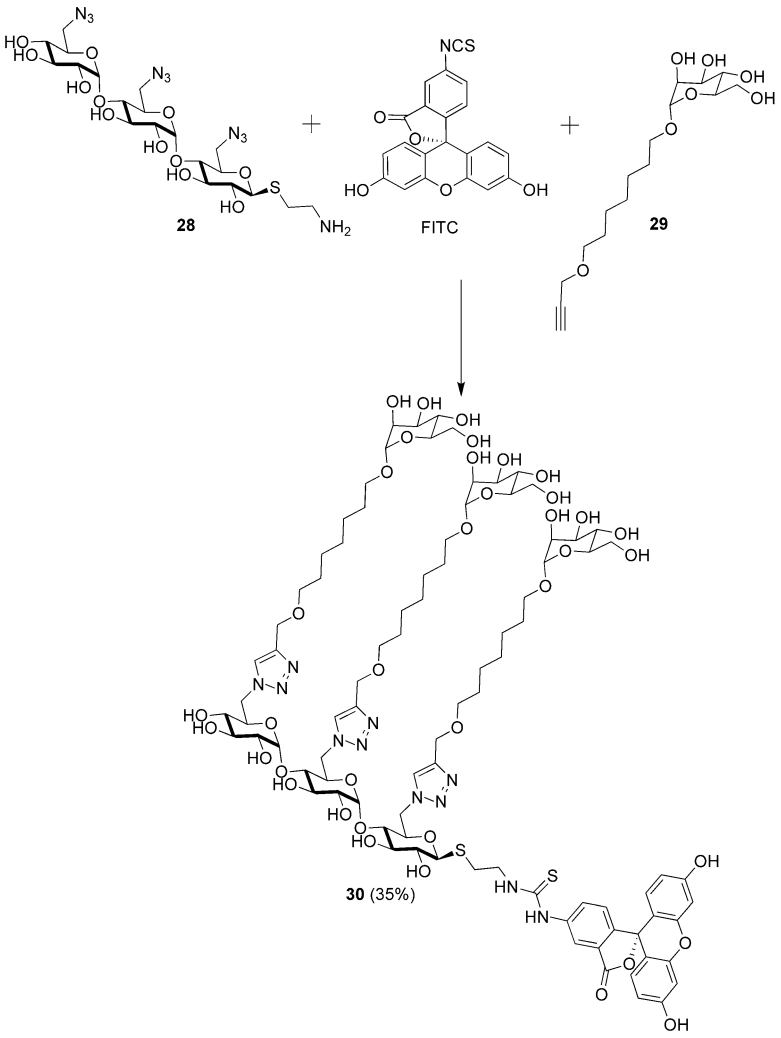

Scheme 6. Synthesis of probe **30**.

well averaged out and has a small standard error (Table 2). Dynamic protein–protein contacts could thus be the cause of variations in the baseline at equilibrium (Figure 1, compound **27**) and could potentially trigger bacterial clustering as well.

Thermodynamic parameters revealed an almost perfect addition of enthalpies for FimH occupation upon the addition of every other mannoside going from the monovalent **24** to the heptavalent **27** (Table 2). The gain in enthalpy with every other binding site in the compounds with increasing valencies ($n=1$, 2, 3, or 7) is almost perfectly compensated for the loss of entropy by partial enthalpy–entropy compensation (Figure 2). The affinities of the four compounds **24**–**27** thus appear highly correlated (Table 2, Figure 2).

To understand this effect and discern the individual contributions to affinity of the subsequently bound mannosides on the multivalent ligands, we set up reverse titrations. In our reverse titration method, FimH is titrated through the needle in high concentrations and small volumes into the measurement cell that contains the diluted compound. Fitting of FimH binding to sequential binding sites on the multivalent mannosidic ligand renders the same thermodynamic parameters of entropy and enthalpy as in direct titration; however, this time can be measured per individual binding site. Ideally, this delivers a microscopic affinity constant per binding site on the ligand.[46] Reverse titration can as such reveal positive, negative or noncooperativity between sequential binding sites.[47]

The reverse titration experiments yielded reliable data only for the divalent HM ligand **25** (Figure 3). It was possible to derive interesting thermodynamic information from the reverse titration experiment with the low valency compound **25**. FimH displays a higher affinity for the first binding event on **25** ($K_d=7.6$ nM, Figure 2) than for the monovalent **24** (14.4 nM, Table 1). A higher microscopic affinity is indeed expected for the binding of the first ligand on a multivalent glycoconjugate than for the same ligand on a monovalent glycoconjugate because of an increased probability of binding.[47] On the other hand, the affinity for the second binding site on a multivalent glycoconjugate is by definition lower than for the first one in the absence of cooperativity due to the decreased number of potential binding sites.[47] The large dump in affinity of FimH for the second binding site of **25** is more significant than this statistical effect. Fitting or the reverse titration indicates negative cooperativity between the two sequential binding sites of **25** (Table 2, Figures 2 and 3).

Fluorescence microscopy: We decided to modify trivalent **26** for the microscopy experiments, as this compound was a good compromise in view of its high inhibitory potency in both ITC and HAI. Fluorescent microscopy experiments were performed with FITC-labeled compound **30** and fluorescently labeled bacteria with Hoechst 33258. A homogenous solution of disperse bacteria was observed in the absence of glycoconjugate **30** (Figure 4a). When the sugar **30** was added at a concentration of 4 μM, clusters of bacteria were formed (Figure 4b). The green in the cluster unambiguously indicated the presence of **30** in the middle of the bacterial cluster. These results showed that the formation of the

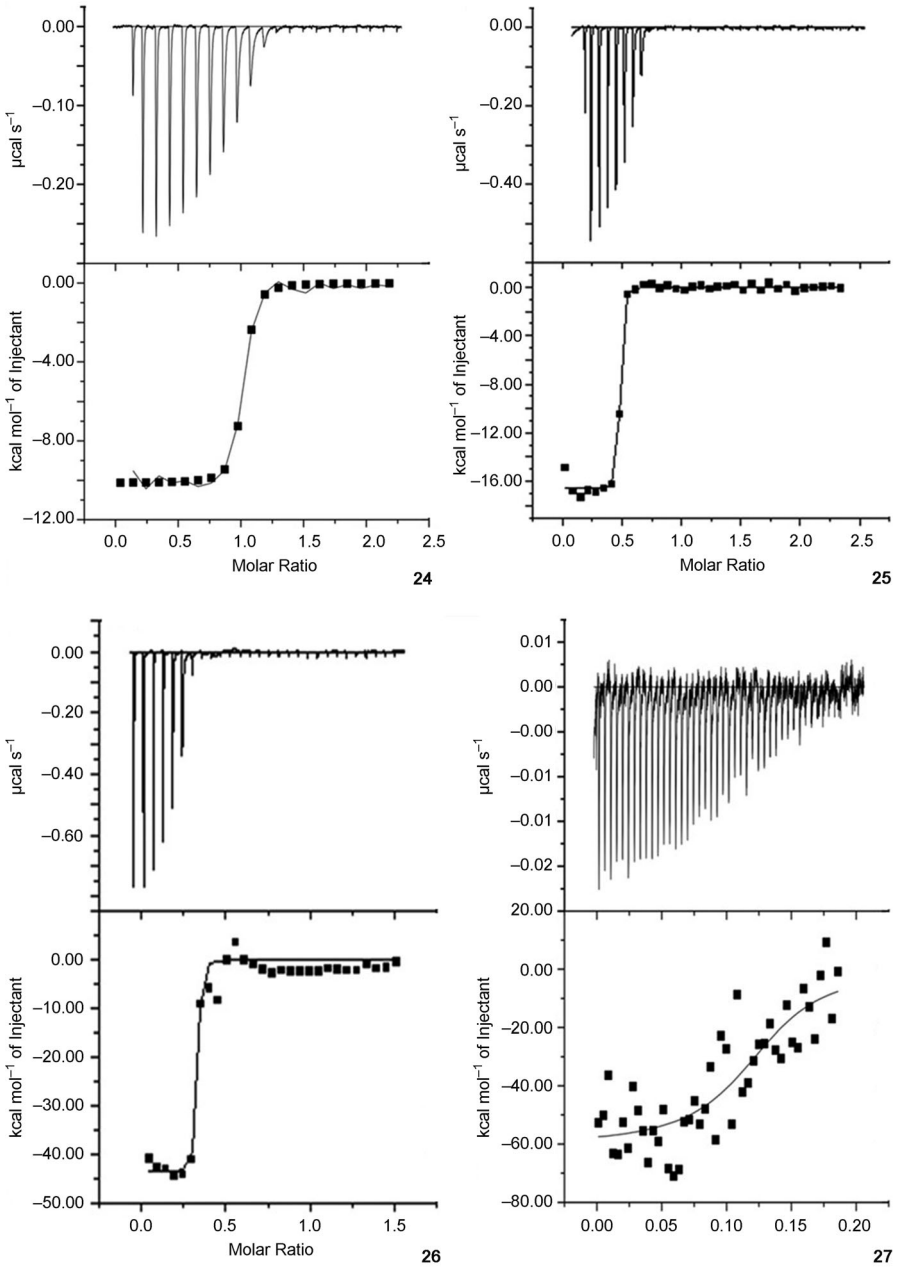

Figure 1. ITC raw data and fittings of the multivalent ligands.

bacterial clusters is promoted by the trivalent glycoconjugate **30**. Previous papers reported on the possibility to cluster bacteria with polymeric glycoconjugates that bear a large number of lectin ligands.[15,16]

Seeberger and co-workers have grafted mannosides on a rigid poly(*p*-phenylene ethynylene) (PPE) core for the aggregation and fluorescent detection of bacteria in solution.[15] Alexander and co-workers have shown the possibility to control bacterial aggregation with thermoresponsive polymer chains.[16] As far as we know, the possibility to promote *E. coli* clustering with low valency ligands, such as the trimeric compound **30** here, has not been previously reported. Thus, our results indicate for the first time that a trivalent ligand with short spacers can promote cross-linking of FimH that belong to different bacteria.

Conclusion

We have developed an efficient synthetic methodology to design water-soluble ligands with valencies that range from 1 to 7. We repeated a critical glucoside fragment to build regular structures for a strict assessment of potential multivalent effects. An amino group was also introduced in the anomeric position of the scaffolds for further grafting of a fluorescent probe. Alternatively, we also developed a rapid one-pot procedure to tether simultaneously the HM epitopes and FITC onto the carbohydrate core. The set of ligands designed are strong inhibitors of FimH and display nanomolar affinity for the isolated FimH lectin domain in solution, as evidenced by ITC experiments.

Insights into the binding-mode operation were also provided by ITC experiments. Considering that a chelate effect is not expected due to the monomeric nature of FimH, the affinity enhancement observed can be either ascribed to intrinsic multivalent effects,[20b,48] in which the proximity of the tethered epitopes allow their subsequent binding and recapture by a unique FimH molecule, or to an aggregative process, in which a multivalent ligand can bind to several receptors simultaneously. ITC data are clearly indicative of the second mechanism by showing that all the structural binding epitopes of the multivalent ligands were saturated by FimH molecules. The strong binding affinity of HM for the FimH receptor may limit the recapture mechanism from operating during intrinsic multivalent effects.

Negative cooperativity between the sequential binding sites on the multivalent HM ligands reduces the affinity of FimH in the ITC experiments. This may be caused by steric hindrance between the FimH lectin domains that are bound tightly and closely together onto a relatively small carbohy-

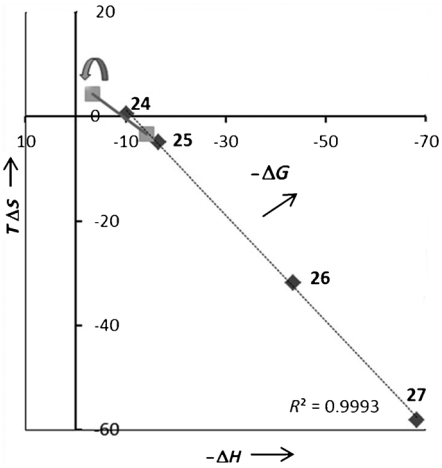

Figure 2. (◆) Direct titration experiments showed a strong enthalpy–entropy compensation ($R^2=0.9993$) for the multivalent interaction of the monomeric FimH lectin domain with compounds with structural and functional valencies (n) of 1 (**24**), 2 (**25**), 3 (**26**), and 7 (**27**). (■) Reverse titration of **25** shows a deviation from the thermodynamic enthalpy–entropy compensation axis for the second binding site of the divalent glycoconjugate **25**, thus demonstrating negative cooperativity between sequential mannose epitopes (see Table 2).

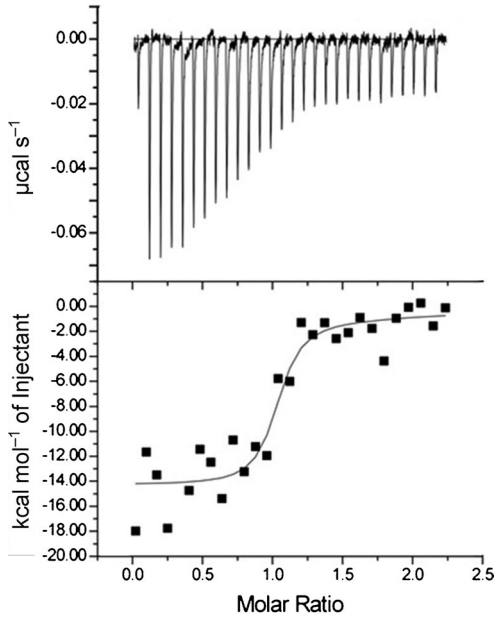

Figure 3. Reverse titration of FimH (21.3 µM) into divalent ligand **25** (2 µM) (22.1503 °C). From the previous observation that each of the two binding sites on **25** can fully occupy a FimH molecule, the molar ratio per sequential binding sites had been fixed to 1 in the fitting of sequential binding to the first ($K_d=(7.6\pm14.4)$ nM) and the second ($K_d=(2.1\pm7.7)$ µM) mannoside epitope.

drate scaffold. We could confirm that these apparent FimH lectin microaggregates grow according to the structural valency of the HM ligands by the determination of functional stoichiometric ratios in direct titration calorimetry. A significant binding improvement due to valency of the ligand was, however, observed in the inhibition of haemagglutination by

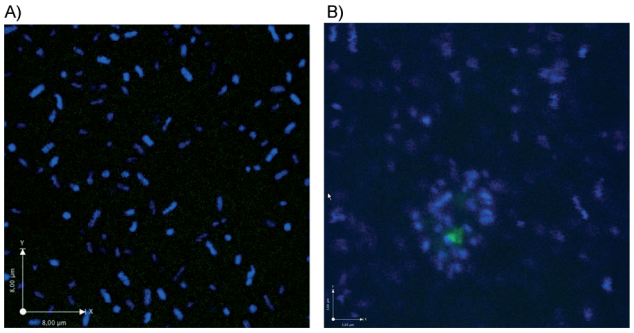

Figure 4. Laser scanning microscopy images of A) Uropathogenic *E. coli* in solution fluorescently labeled with Hoechst stain 33258. Individual bacteria are observed without clustering; scale bar 8.00 µm. B) Bacterial cluster (in blue) co-localizes with FITC-labeled **30** (green); scale bar 3.60 µm.

uropathogenic *E. coli*. Multivalent inhibitors that surpass the potency of HM were observed in this assay.

Furthermore, fluorescence microscopy evidenced that the trivalent ligand **30** was able to promote bacterial clustering, a phenomenon that is not accessible to monovalent ligands, but that has previously been reported with polymeric glycoconjugates.

These results show that rather simple ligands with low valencies are efficient chemical tools for capturing living bacteria in solution.

Experimental Section

General procedures: All purchased materials were used without further purification. Dichloromethane and DMF were distilled from calcium hydride, pyridine over KOH, and tetrahydrofuran over sodium and benzophenone. Analytical thin-layer chromatography (TLC) was carried out using Merck D.C.-Alufolien Kieselgel 60 F_{254}. Flash chromatography (FC) was performed using GEDURAN SI 60, 0.040–0.060 mm pore size, using distilled solvents. ^{1}H and ^{13}C nuclear magnetic resonance (NMR) spectra were respectively recorded at 300 and 75.5 MHz using a Bruker AC-300 or at 600 and 150 MHz using a Bruker AC-600 spectrometer, and chemical shifts are reported in parts per million relative to tetramethylsilane or a residual solvent peak peak ($CHCl_3$: ^{1}H: $\delta=7.26$ ppm, ^{13}C: $\delta=77.2$ ppm; [D_6]DMSO: ^{1}H: $\delta=2.54$ ppm, ^{13}C: $\delta=40.4$ ppm). Peak multiplicity is reported as: singlet (s), doublet (d), triplet (t), quartet (q), pentet (p), sixtet (s), multiplet (m), and broad (br). High-resolution mass spectra HRMS were obtained by electrospray ionization (ESI) using a Micromass-Waters Q-TOF Ultima Global instrument. Optical rotations were measured using a 343 Perkin–Elmer instrument at 20 °C in a 1 cm cell in the stated solvent; $[\alpha]_D$ values are given in 10^{-1} °cm^{-1}g^{-1} (concentration c given as g100 mL^{-1}). Microwave irradiation was performed using a CEM Discover apparatus (300 W). Preparative reversed-phase HPLC was carried out using a Waters PREP LC 4000 chromatography system with a (DEDL) PL-ELS 1000 photodiode array detector. All HPLC samples were purified using a preparative Prevail C-18 column (2.2×25 cm). The mobile phase was H_2O (solvent A) and MeOH (solvent B). For method A: The mobile phase was H_2O (solvent A) and MeOH (solvent B). The gradient consisted of 5% A for 5 min to 100% B in 55 min (22.0 mL min^{-1} flow rate). For method B: The mobile phase was H_2O (solvent A) and MeOH (solvent B). The gradient consisted of 5% A for 5 min to 100% B in 55 min (22.0 mL min^{-1} flow rate).

Procedure for the thioglycosylations: Compound **13** (1.20 g, 1.18 mmol), compound **15** (1.76 g, 5.9 mmol), and activated 4 Å molecular sieves

(2.00 g) were dissolved in dry dichloromethane (5 mL). The mixture was stirred at −20 °C for 30 min under argon atmosphere, and TMSOTf (71 μL, 0.39 mmol) was added. After 15 min of stirring, $NaHCO_3$ was added (70 mg), and the mixture filtered and evaporated under reduced pressure. The residue was subjected to chromatography on silica gel with ethyl acetate/cyclohexane (8:2 to 6:4) to afford **18** (700 mg, 55 %).

Procedure for the microwave-assisted cyclization: Compound **18** (100 mg, 0.09 mmol), compound **20** (140 mg, 0.28 mmol), $CuSO_4$ (21 mg, 0.13 mmol), and sodium ascorbate (21 mg, 0.26 mmol) were dissolved in a mixture of dioxane (2 mL) and water (0.5 mL) The mixture was stirred under microwave irradiation at 70 °C for 30 min. After evaporation to dryness, the residue was dissolved in dichloromethane (5 mL) and filtered. The filtrate was evaporated to dryness, and the mixture was subjected to chromatography on a silica gel column with ethyl acetate/cyclohexane (8:2) to methanol/ethyl acetate (1:9) as eluent to afford **23** (181 mg, 76 %).

Procedure for the deprotection of acetates and Fmoc groups: Compound **23** (150 mg, 0.05 mmol) was dissolved in a 7 N solution of ammonia in methanol (20 mL) and the mixture was stirred at room temperature for 24 h. After evaporation under reduced pressure, the residue was dissolved in diethyl ether (10 mL) and water (10 mL). The aqueous phase was extracted with diethyl ether (2×20 mL) and evaporated under reduced pressure. The residue was purified by HPLC with conditions A to afford **26** (62 mg, 76 %).

Glycoconjugate 24: $[\alpha]_D^{20} = +101$ ($c = 1$ in H_2O); ^{1}H NMR (600 MHz, D_2O): $\delta = 8.00$ (s, 1H; $H_{triazole}$), 4.80 (d, $J = 1$ Hz, 1H; H-1_{HM}), 4.56 (m, 2H; O-CH_2-triazole), 4.48 (d, $J = 10$ Hz, 1H; H-1), 3.85–3.40 (m, 16H; H-2, H-2_{HM}, H-3, H-3_{HM}, H-4, H-4_{HM}, H-5, H-5_{HM}, 2×H-6, 2×H-6_{HM}, 2×CH_2O), 2.99–2.60 (m, 4H; CH_2-S, CH_2-NH_2), 1.50–1.23 ppm (m, 10H; 5×CH_2); ^{13}C NMR (150 MHz, D_2O): $\delta = 142.3$ (*C*=$CH_{triazole}$), 125.8 (*C*H=$C_{triazole}$), 99.6 (C-1_{HM}), 85.3 (C-1), 77.5, 77.4, 76.9, 76.8, 72.7, 71.9, 70.9, 70.8, 70.6, 70.5, 70.3, 70.1, 67.8, 66.7 (C-2, C-3, C-4, C-5, C-2_{HM}, C-3_{HM}, C-4_{HM}, C-5_{HM}, CH_2O), 61.8 (O-CH_2-triazole), 60.9 (C-6_{HM}), 51.1 (C-6), 39.4, 39.3, 38.2, 38.1, 37.9, 37.7, 37.6, 36.9 (CH_2-NH_2, CH_2), 31.4 ppm (CH_2-S); HRMS (ES+): *m*/*z* calcd for $C_{24}H_{44}N_4O_{11}SH$: 597.2806; found: 597.2820.

Glycoconjugate 25: $[\alpha]_D^{20} = +112$ ($c = 1$ in H_2O); ^{1}H NMR (600 MHz, D_2O): $\delta = 7.96$, 7.82 (s, 2H; 2×$H_{triazole}$), 5.25 (d, $J = 4.0$ Hz, 1H; H-1^{II}), 4.75 (d, $J = 1$ Hz, 2H; 2×H-1_{HM}), 4.45 (m, 2H; O-CH_2-triazole), 4.15 (m, 2H; O-CH_2-triazole), 4.48 (d, $J = 10$ Hz, 1H; H-1), 3.85–3.40 (m, 16H; H-2^{I-II}, 2×H-2_{HM}, H-3^{I-II}, 2×H-3_{HM}, H-4^{I-II}, 2×H-4_{HM}, H-5^{I-II}, 2×H-5_{HM}, 2×H-6^{I-II}, 4×H-6_{HM}, 4×CH_2O), 2.65–2.30 (m, 4H; CH_2-S, CH_2-NH_2), 1.57–1.13 ppm (m, 20H; 10×CH_2); ^{13}C NMR (150 MHz, D_2O): $\delta = 144.1$, 144.0 (2×*C*=$CH_{triazole}$), 126.1, 125.7 (2×*C*H=$C_{triazole}$), 100.9, 99.6 (2×C-1_{HM}), 85.2 (C-1), 80.7, 76.9, 75.4, 72.6, 72.4, 72.0, 71.7, 71.5, 70.9, 70.6, 70.5, 70.0, 67.8, 66.6 (C-2^{I-II}, C-3^{I-II}, C-4^{I-II}, C-5^{I-II}, C-2_{HM}, C-3_{HM}, C-4_{HM}, C-5_{HM}, CH_2O), 62.3, 62.2 (O-CH_2-triazole), 61.7, 60.9 (C-6_{HM}), 51.4, 50.4 (C-6^{I-II}), 39.9, 31.4, 31.2, 28.6, 28.4, 28.3, 28.2, 25.3, 25.2, 25.1 ppm (CH_2-NH, CH_2-S, CH_2); HRMS (ES+): *m*/*z* calcd for $C_{46}H_{81}N_7O_{22}SH$: 1116.5233; found: 1116.5264.

Glycoconjugate 26: $[\alpha]_D^{20} = +120$ ($c = 1$ in H_2O); ^{1}H NMR (600 MHz, D_2O) $\delta = 7.96$, 7.89, 7.82 (s, 3H; 3×$H_{triazole}$), 5.25, 5.15 (2d, $J = 4$ Hz, 2H; H-1^{II-III}), 4.59 (d, $J = 1$ Hz, 3H; 3×H-1_{HM}), 4.28 (d, $J = 10$ Hz, 1H; H-1), 4.20–3.96 (m, 6H; 3×O-CH_2-triazole), 3.85–3.10 (m, 42H; H-2 $^{I-III}$, 3×H-2_{HM}, H-3^{I-III}, 3×H-3_{HM}, H-4^{I-III}, 3×H-4_{HM}, H-5^{I-III}, 3×H-5_{HM}, 2×H-6^{I-III}, 6×H-6_{HM}, 6×CH_2O), 2.55–2.35 (m, 4H; CH_2-S, CH_2-NH_2), 1.57–1.13 ppm (m, 30H; 15×CH_2); ^{13}C NMR (150 MHz, D_2O): $\delta = 144.1$, 144.0, 143.9 (C=$CH_{triazole}$), 125.7 (CH=$C_{triazole}$), 99.6 (C-1_{HM}), 85.2 (C-1^I), 80.9, 76.8, 75.1, 72.6, 72.3, 72.2, 71.6, 71.5, 71.0, 70.9, 70.7, 70.6, 70.5, 70.1, 69.8, 67.7, 66.6 (C-2^{I-III}, C-3^{I-III}, C-4^{I-III}, C-5^{I-III}, C-2_{HM}, C-3_{HM}, C-4_{HM}, C-5_{HM}, CH_2O), 62.6, 62.4, 62.2, 61.7, 60.8 (O-CH_2-triazole, C-6_{HM}), 50.7, 50.2 (C-6^{I-III}), 39.8, 36.8, 31.2, 28.6, 28.4, 28.4, 28.3, 28.2, 25.3, 25.3, 25.2, 25.1 ppm (CH_2-NH, CH_2-S, CH_2); HRMS (ES+): *m*/*z* calcd for $C_{68}H_{118}N_{10}O_{33}SNa$: 1657.7482; found: 1657.7470.

Glycoconjugate 27: $[\alpha]_D^{20} = +98$ ($c = 1$ in H_2O); ^{1}H NMR (600 MHz, D_2O) $\delta = 7.90$, 7.70 (s, 7H; 7×$H_{triazole}$); 5.12 (7d, $J = 4$ Hz, 7H; H-1^{II-VII}), 5.00–3.01 (m, 134H; H-1^I, 7×H-1_{HM}, H-2^{I-VII}, 7×H-2_{HM}, H-3^{I-VII}, 7×H-3_{HM}, H-4^{I-VII}, 7×H-4_{HM}, H-5^{I-VII}, 7×H-5_{HM}, 2×H-6^{I-VII}, 14×H-6_{HM}, 14×CH_2O, 7×O-CH_2-triazole), 2.95–2.35 (m, 4H; CH_2-S, CH_2-NH_2), 1.57–1.13 (m, 70H, 35×CH_2); ^{13}C NMR (150 MHz, D_2O): $\delta = 144.0$ (7×C=$CH_{triazole}$), 126.1 (7×CH=$C_{triazole}$), 101.42, 101.05 (C-1^{II-VII}), 99.7 (7×C-1_{HM}), 85.6 (C-1^I), 81.4, 76.8, 72.6, 71.6, 71.2, 70.7, 70.6, 70.5, 70.2, 69.7, 67.6, 66.6 (C-2^{I-VII}, C-3^{I-VII}, C-4^{I-VII}, C-5^{I-VII}, C-2_{HM}, C-3_{HM}, C-4_{HM}, C-5_{HM}, CH_2O), 62.4, 61.7, 60.8 (7×O-CH_2-triazole, 7×C-6_{HM}); 51.6, 50.6 (C-6^{I-VII}), 39.2, 36.9, 31.4, 28.7, 28.7, 28.5, 28.4, 27.4, 25.5, 25.1, 25.0 (CH_2-NH, CH_2-S, CH_2); HRMS (ES+): *m*/*z* calcd for $C_{156}H_{263}N_{22}O_{77}SNa_3F$: 3734.7192; found: 3734.7242.

Procedure for the one-pot synthesis of 30: Compound **18** (20 mg, 0.02 mmol) was dissolved in a 7 N solution of ammonia in methanol (10 mL) and the mixture was stirred at room temperature for 24 h. After evaporation under reduced pressure, the residue was dissolved in diethyl ether (10 mL) and water (10 mL). The aqueous phase was extracted with diethyl ether (2×20 mL) and evaporated under reduced pressure. Compound **20** (30 mg, 0.06 mmol) was dissolved in a 7 N solution of ammonia in methanol (10 mL), and the mixture was stirred at room temperature for 24 h. After evaporation under reduced pressure, the residue was dissolved in diethyl ether (10 mL) and water (10 mL). The aqueous phase was extracted with diethyl ether (2×20 mL) and evaporated under reduced pressure. The two crude products, fluorescein isothiocyanate (12 mg, 0.03 mmol), $CuSO_4$ (7 mg, 0.015 mmol), and sodium ascorbate (10 mg, 0.030 mmol) were dissolved in DMF (4 mL) and water (1 mL). The mixture was stirred in a dark room at room temperature for 24 h. After evaporation to dryness, the residue was diluted in water and extensively washed with EtOAc. After lyophilization, the mixture was purified by HPLC with B conditions to afford **30** (9 mg, 35 %, $t_r = 25$ min).

Isothermal titration calorimetry (ITC): The FimH adhesin lectin domain was expressed and purified as previously described and finally dialyzed against 20 mM 4-(2-hydroxyethyl)-1-piperazineethanesulfonic acid (HEPES) pH 7.4 with 150 mM NaCl.[11] The last change of dialysis buffer was filter-sterilized and kept as buffer to dilute FimH and compounds for the calorimetry. A VP-ITC (Microcal) instrument was used for both direct and reverse titrations; 280 μL was always injected into the 1.4 mL measurement cell. Respective concentrations and molar ratios in needle and cell, injection volumes, and time intervals between injections were varied to obtain 1) inflection and saturation about halfway through the experiment, 2) sufficient heat production per injection to allow good peak integration, and 3) sufficient time between the injections to allow a return to equilibrium. The concentrations used in every ITC experiment are given in the Supporting Information. Stirring speed of the needle was always 307 rpm. Fitting was performed using the Origin software using the equations for one set of binding sites in the direct titration fittings, or for sequential binding sites for the reverse titration fittings.

Inhibition of haemagglutination (HAI): Inhibition of guinea pig red blood cell haemagglutination by the type-1 piliated uropathogenic *E. coli* strain UTI89 by the newly synthesized glycoconjugates **24**–**27**. A twofold dilution of glycoconjugates was prepared in HEPES (25 μL; 20 mM; pH 7.4) with NaCl (150 mM), starting from 1 mM as the highest concentration. UTI89 *E. coli* were grown statically overnight in Luria-Bertani medium at 37 °C, washed three times in ice-cold phosphate-buffered saline, and resolubilized. The bacterial solution (25 μL) was added to the twofold dilution series of the compound. Finally, guinea pig red blood cells (50 μL), washed in buffer and diluted to 5 %, were added to a final 100 μL and left on ice for 30 min before readout.

Fluorescence microscopy: UTI189 *E. coli* strains were grown statically overnight in LB at 37 °C, washed and diluted in PBS buffer (NaCl: 137 mM, KCl: 2.7 mM, Na_2HPO_4: 10 mM, K_2HPO_4: 1.76 mM; pH 7.4). Labeled trisaccharide **30** (4 μM) was diluted in buffer and poured into the bacteria solution. Fluorescence microscopy and digital image acquisition and analysis were performed using a Leica TCS SP5 AOBS fluorescence microscope.

Acknowledgements

This work was carried out with financial support from the French Agence Nationale de la Recherce (ANR JC07_183019), the Centre Na-

tional de la Recherche Scientifique, the Ministère Délégué à l'Enseignement Supérieur et à la Recherche, and the Conseil Régional de Picardie.

[1] For a review, see: A. J. Alanis, *Arch. Med. Res.* **2005**, *36*, 697–705.
[2] H. W. Boucher, G. H. Talbot, J. S. Bradley, J. E. Edwards, D. Gilbert, L. B. Rice, M. Scheld, B. Spellberg, J. Bartlett, *Clin. Infect. Dis.* **2009**, *48*, 1–12.
[3] K. K. Kumarasami, M. A. Toleman, T. R. Walsh, J. Bagaria, F. Butt, R. Balakrishnan, U. Chaudhary, M. Doumith, C. G. Giske, S. Irfan, P. Krishnan, A. V. Kumar, S. Maharjan, S. Mushtaq, T. Noorie, D. L. Paterson, A. Pearson, C. Perry, R. Pike, B. Rao, U. Ray, J. B. Sarma, M. Sharma, E. Sheridan, M. A. Thirunarayan, J. turton, S. Upadhyay, M. Warner, W. Welfare, D. M. Livermore, N. Woodford, *Lancet Infect. Dis.* **2010**, *9*, 578–579.
[4] For an overview, see: a) R. J. Pieters, *Med. Res. Rev.* **2007**, *27*, 796–816; b) R. J. Pieters, *Org. Biomol. Chem.* **2009**, *7*, 2013–2025; c) A. Imberty, Y. M. Chabre, R. Roy, *Chem. Eur. J.* **2008**, *14*, 7490–7499; d) Y. M. Chabre, R. Roy, *Adv. Carbohydr. Chem. Biochem.* **2010**, *63*, 165–393; e) D. Deniaud, K. Julienne, S. G. Gouin, *Org. Biomol. Chem.* **2011**, *9*, 966–979.
[5] Y. C. Lee, R. T. Lee, *Acc. Chem. Res.* **1995**, *28*, 321–327.
[6] a) N. Firon, I. Ofek, N. Sharon, *Carbohydr. Res.* **1983**, *120*, 235–249; b) N. Firon, I. Ofek, N. Sharon, *Infect. Immun.* **1984**, *43*, 1088–1090.
[7] T. K. Lindhorst, S. Kötter, J. Kubisch, U. Krallmann-Wenzel, S. Ehlers, V. Kren, *Eur. J. Org. Chem.* **1998**, 1669–1674.
[8] a) M. Touaibia, A. Wellens, T. C. Shiao, Q. Wang, S. Sirois, J. Bouckaert, R. Roy, *ChemMedChem* **2007**, *2*, 1190–1201; b) M. Touaibia, T. C. Shiao, A. Papadopoulos, J. Vaucher, Q. Wang, K. Benhamioud, R. Roy, *Chem. Commun.* **2007**, 380–382.
[9] Z. Han, J. S. Pinkner, B. Ford, R. Obermann, W. Nolan, S. A. Wildman, D. Hobbs, T. Ellenberger, C. K. Cusumano, S. J. Hultgren, J. W. Janetka, *J. Med. Chem.* **2010**, *53*, 4779–4792.
[10] J. Bouckaert, J. Berglund, M. Schembri, E. De Genst, L. Cools, M. Wuhrer, C-S. Hung, J. Pinkner, R. Slättegård, A. Zavialov, D. Choudhury, S. Langermann, S. J. Hultgren, L. Wyns, P. Klemm, S. Oscarson, S. D. Knight, H. De Greve, *Mol. Microbiol.* **2004**, *55*, 441–455.
[11] A. Wellens, C. Garofalo, H. Nguyen, N. Van Gerven, R. Slättegård, P. Hernalsteens, L. Wyns, S. Oscarson, S. De Greve, S. Hultgren, J. Bouckaert, *PLoS ONE* **2008**, *3*, e2040.
[12] N. Nagahori, R. T. Lee, S.-I. Nishimura, D. Pagé, R. Roy, Y. C. Lee, *ChemBioChem* **2002**, *3*, 836–844.
[13] C.-C. Lin, Y.-C. Yeh, C.-Y. Yang, C.-L. Chen, G.-F. Chen, C.-C. Chen, Y.-C. Wu, *J. Am. Chem. Soc.* **2002**, *124*, 3508–3509.
[14] B.-S. Kim, W.-Y. Yang, J.-H. Ryu, Y.-S. Yoo, M. Lee, *Chem. Commun.* **2005**, 2035–2037.
[15] M. D. Disney, J. Zheng, T. M. Swager, P. H. Seeberger, *J. Am. Chem. Soc.* **2004**, *126*, 13343–13346.
[16] G. Pasparakis, A. Cockayne, C. Alexander, *J. Am. Chem. Soc.* **2007**, *129*, 11014–11015.
[17] C. C. M. Appeldoorn, J. A. F. Joosten, F. Ait el Maate, U. Dobrindt, J. Hacker, R. M. J. Liskamp, A. Salam Khan, R. J. Pieters, *Tetrahedron. Asymmetry* **2005**, *16*, 361–372.
[18] S. G. Gouin, A. Wellens, J. Bouckaert, J. Kovensky, *ChemMedChem* **2009**, *4*, 749–755.
[19] S. G. Gouin, E. Vanquelef, J.-M. García Fernández, C. Ortiz Mellet, F.-Y. Dupradeau, J. Kovensky, *J. Org. Chem.* **2007**, *72*, 9032–9045.
[20] a) J. M. Benito, M. Gómez-García, C. Ortiz Mellet, I. Baussanne, J. Defaye, J. M. García Fernández, *J. Am. Chem. Soc.* **2004**, *126*, 10355–10366; b) M. Gómez-García, J. M. Benito, D. Rodríguez-Lucena, J.-X Yu, K. Chmurzky, C. Ortiz Mellet, R. Gutiérrez Gallego, A. Maestre, J. Defaye, J. M. García Fernández, *J. Am. Chem. Soc.* **2005**, *127*, 7970–7971.
[21] a) C. D. Heidecke, T. K. Lindhorst, *Chem. Eur. J.* **2007**, *13*, 9056–9067; b) O. Sperling, M. Dubber, T. K. Lindhorst, *Carbohydr. Res.* **2007**, *342*, 696–703; c) M. Dubber, O. Sperling, T. K. Lindhorst, *Org. Biomol. Chem.* **2006**, *4*, 3901–3902; d) M. Dubber, T. K. Lindhorst, *J. Org. Chem.* **2000**, *65*, 5275–5281.
[22] J. J. Garcia-López, F. Hernández-Mateo, J. Isac-García, J. M. Kim, R. Roy, F. Santoyo-González, A. Vargas-Berenguel, *J. Org. Chem.* **1999**, *64*, 522–531.
[23] a) V. V. Rostovtsev, L. G. Green, V. V. Fokin, K. B. Sharpless, *Angew. Chem.* **2002**, *114*, 2708–2711; *Angew. Chem. Int. Ed.* **2002**, *41*, 2596–2599; b) C. W. Tornøe, C. Christensen, M. Meldal, *J. Org. Chem.* **2002**, *67*, 3057–3064.
[24] For reviews, see: a) V. D. Bock, H. Hiemstra, J. H. van Maarseveen, *Eur. J. Org. Chem.* **2006**, 51–68; b) S. Dedola, S. A. Negopodiev, R. A. Field, *Org. Biomol. Chem.* **2007**, *5*, 1006–1017; c) M. Meldal, C. W. Tornøe, *Chem. Rev.* **2008**, *108*, 2952–3015.
[25] a) A. Díaz-Moscoso, A. Méndez-Ardoy, F. Ortega-Caballero, J. M. Benito, C. Ortiz Mellet, J. Defaye, T. M. Robinson, A. Yohannes, V. A. Karginov, J. M. García Fernández, *ChemMedChem* **2011**, *6*, 181–192; b) S. Srinivasachari, K. M. Fichter, T. M. Reineke, *J. Am. Chem. Soc.* **2008**, *130*, 4618–4627; c) S. G. Gouin, L. Bultel, C. Falentin, J. Kovensky, *Eur. J. Org. Chem.* **2007**, 1160–1167; d) S. Cecioni, V. Oerthel, J. Iehl, M. Holler, D. Goyard, J.-P. Praly, A. Imberty, J.-F. Nierengarten, S. Vidal, *Chem. Eur. J.* **2011**, *17*, 3252–3261.
[26] a) J. Diot, M. I. Garcia-Moreno, S. G. Gouin, C. Ortiz Mellet, K. Haupt, J. Kovensky, *Org. Biomol. Chem.* **2009**, *7*, 357–363; b) P. Compain, C. Decroocq, J. Iehl, M. Holler, D. Hazelard, T. Mena Barragán, C. Ortiz Mellet, J. F. Nierengarten, *Angew. Chem.* **2010**, *122*, 5889–5892; *Angew. Chem. Int. Ed.* **2010**, *49*, 5753–5756.
[27] V. Maunier, P. Boullanger, D. Lafont, Y. Chevalier, *Carbohydr. Res.* **1997**, *299*, 49–57.
[28] S. G. Gouin, J. Kovensky, *Tetrahedron Lett.* **2007**, *48*, 2875–2879.
[29] J. L. Jiménez-Blanco, J. M. García Fernández, A. Gadelle, J. Defaye, *Carbohydr. Res.* **1997**, *303*, 367–372.
[30] a) N. Thiebault, D. Lesur, P. Godé, V. Moreau, F. Djedaïni-Pilard, *Carbohydr. Res.* **2008**, *343*, 2719–2728; b) D. Lesur, PhD Thesis, Université de Picardie Jules Verne (France), **2004**.
[31] A. R. Khan, V. T. D'Souza, *J. Org. Chem.* **1994**, *59*, 7492–7495.
[32] a) A. Gadelle, J. Defaye, *Angew. Chem.* **1991**, *103*, 94–95; *Angew. Chem. Int. Ed. Engl.* **1991**, *30*, 78–80; b) K. Chmurski, J. Defaye, *Tetrahedron Lett.* **1997**, *38*, 7365–7368.
[33] B. I. Gorin, R. J. Riopelle, G. R. J. Thatcher, *Tetrahedron Lett.* **1996**, *37*, 4647–4650.
[34] D. Lesur, A. Gassama, V. Moreau, S. Pilard, F. Djedaïni-Pilard, *Carbohydr. Res.* **2005**, *340*, 1225–1231.
[35] N. Sakairi, K. Matsui, H. Kuzuhara, *Carbohydr. Res.* **1995**, *266*, 263–268.
[36] E. Farkas, L. Jánossy, J. Harangi, L. Kandra, A. Lipták, *Carbohydr. Res.* **1997**, *303*, 407–415.
[37] E. Bourgeaux, J.-C. Combret, *Tetrahedron: Asymmetry* **2000**, *11*, 4189–4205.
[38] B. Hoffmann, D. Zanini, I. Ripoche, R. Bürli, A. Vasella, *Helv. Chim. Acta* **2001**, *84*, 1862–1888.
[39] A. Kikuzawa, T. Kida, Y. Nakatsuji, M. Akashi, *J. Org. Chem.* **2005**, *70*, 1253–1261.
[40] A. Bösch, P. Mischnick, *Biomacromolecules* **2007**, *8*, 2311–2320.
[41] Y. Miura, T. Arai, T. Yamagata, *Carbohydr. Res.* **1996**, *289*, 193–199.
[42] S.-S. Weng, Y.-D. Lin, C.-T. Chen, *Org. Lett.* **2006**, *8*, 5633–5636.
[43] N. A. Rodios, *J. Heterocycl. Chem.* **1984**, *21*, 1169–1173.
[44] M. Durka, K. Buffet, J. Iehl, M. Holler, J. F. Nierengarten, J. Taganna, J. Bouckaert, S. P. Vincent, *Chem. Commun.* **2011**, *47*, 1321–1323.
[45] Q. Zhang, Z. Lu, H. Hu, W. Yang, P. E. Marsalek, *J. Am. Chem. Soc.* **2006**, *128*, 9387–9393.
[46] a) T. K. Dam, R. Roy, D. Page, C. F. Brewer, *Biochemistry* **2002**, *41*, 1351–1358; b) T. K. Dam, R. Roy, D. Page, C. F. Brewer, *Biochemistry* **2002**, *41*, 1359–1363.
[47] J. D. Badjic, A. Nelson, S. J. Cantrill, W. B. Turnbull, J. F. Stoddart, *Acc. Chem. Res.* **2005**, *38*, 723–732.
[48] M. S. Quesenberry, R. T. Lee, Y. C. Lee, *Biochemistry* **1997**, *36*, 2724–2732.

Received: February 15, 2011
Revised: June 16, 2011
Published online: July 19, 2011

